International Journal of ISSI, Vol.4 (2007), No. 1,2, pp. 16-23

Dynamic Recrystallization by Necklace Mechanism During Hot Deformation of 316 Stainless Steel

M. Jafari[1], A. Najafizadeh[2*] and J. Rasti[3]
Department of Materials Engineering, Isfahan University of Technology, Isfahan, 84156-83111, Iran

Abstract

The aim of this study is to investigate the nucleation of new grains by necklacing mechanism during dynamic recrystallization (DRX). The material used is 316 stainless steel. In order to modeling the deformation behavior during hot rolling, one-hit compression tests were performed at temperature range of 950-1100 °C with strain rates of 0.01-1s^{-1}. The result shows that at the temperature of 1000 °C with the strain rate of 0.1 s^{-1}, DRX developed by necklace mechanism, it is far from completeness over the steady state stress. By contrast the hardness increased by development of DRX. The final microstructure is very heterogeneous and comprises of very fine and coarse grains due to the occurrence of partial DRX. The results also show that the necklace structure developed by increasing Zener-Hollomon parameter (Z).

Keywords: Dynamic Recrystallization, Necklace Mechanism, 316 Stainless Steel.

1. Introduction

An important process that controls microstructural evolution during hot deformation especially for low stacking fault energy (SFE) alloys is discontinuous dynamic recrystallization (dDRX) [1]. There are two main mechanisms that controlled dynamic nucleation, the first one is the serration of the initial grain boundaries and the other is associated with dynamic recovery (DRV). Serration can be occurring on grain boundaries, deformation band and twin boundaries [2]. Significant nucleation occurs on the deformation bands and twin boundaries when the microstructure has large primary grains size, such as cast materials (more than 200μm) [3]. In wrought products with grains size less than 100 μm, usually nucleation occurs on the grain boundaries.

Typically, the initiation of DRX is preceded by growing fluctuations of the grain boundary shape. Serration and bulges develop, and eventually new grains are generated along these prior grain boundaries by strain induced subboundary formation mechanism. If these new grains are fine and spread predominantly along these prior grain boundaries, at last leads to efficient grain refinement, that is called necklace structure. Figure 1 shows the microstructure development according to the necklace mechanism [4].

Roberts et al. [5] coined the term site saturation for this condition where the nuclei are nucleated at the early stage in the reaction and the initial grain surfaces are completely covered by a shell of DRX grains. This situation occurs just after the first DRX necklace has been formed, so the nucleation rate which is proportional to that area of the pre-existing grain boundaries remaining untransformed becomes vanishingly small. As a result, this mechanism restricts the progress of DRX [6]. Beyond this point, the nucleation rate for static recrystallization (SRX) changes too and so does the growth rate that is limited by the number of nuclei [7].

There is an almost lack of the knowledge on the principles which underlie the expansion of the necklace structure into the deformed volume. Bulging of the new small recrystallized grains requires a very high boundary curvature. This make further nucleation unlikely, because the very high driving force necessary to offset the high surface tension of the bulge is not available in hot deformed microstructures. So, there is some other active mechanism which plays a crucial role for the expansion of the DRX grain through the deformed matrix.

The crucial step for nucleation of DRX in a subgrain structure is the generation of a mobile grain boundary. For small angle grain boundaries, the mobility increases with growing misorientation, but a rotation of 10-15° is commonly assumed to be necessary for nucleation to be occurred. It has been proven that these large misorientations usually were associated with twin boundaries and higher order twin orientations possibly rotated owing to progressive deformation. Thus, continuous subgrain rotation near the large angle boundaries could not be attributed for the expansion of DRX grain through

* *Corresponding author:*
Tel: +98- 311 - 3915742 Fax: +98- 311- 3912752
E-mail: A-najafi@cc.iut.ac.ir
Address: Dept. of Materials Engineering,Isfahan University of Technology, Isfahan, 84156-83111, Iran

1. M.Sc.
2. Professor
3. Ph.D Student

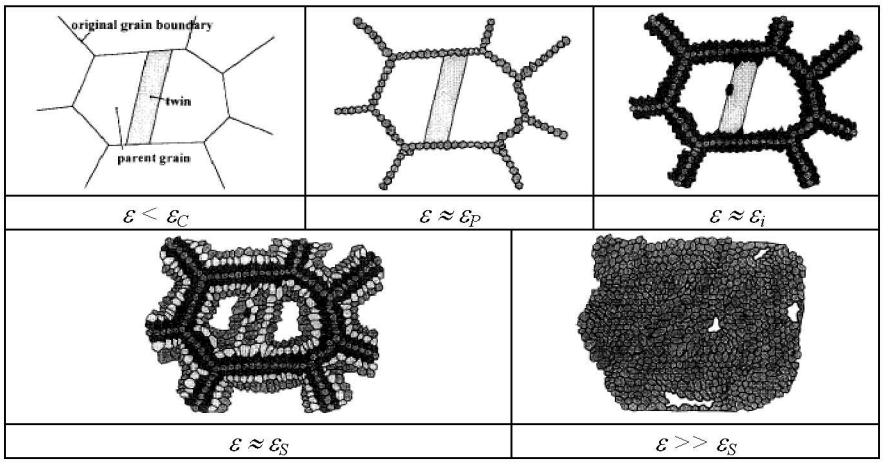

Fig. 1. DRX evolution by necklace mechanism[5].

Table. 1. Chemical composition in wt. % of 316 stainless steel

C	Si	S	P	Mn	Ni	Cr	Mo	Cu
0.043	0.285	0.022<	0.044	1.635	10.225	16.679	2.207	0.489

the deformed matrix. By contrast, the frequency of large misorientation especially in a twin relation inside the subgrain structure is relatively high compared to the frequency of misorientation angles between 10-15° [6].

In the necklace mechanism of the first wave of DRX, new grains form along the initial boundaries, but stop at the specific size, allowing new necklaces of same-size grains to form. So, the DRX grain size down to few microns may promote a dynamic recovery of dislocation evolved by intrinsic slip because of acceleration of dislocation spreading into grain boundaries. Development of this structure by further straining can arise the strain rate sensitivity from typical value of 0.1-0.2 under hot deformation up to 0.3. Such behavior can result from the occurrence of grain boundary sliding on the high dislocation density grain boundaries, which may also lead to a superplastic like flow [4].

Occurrence of DRX in 304 austenitic stainless steel and effects of deformation condition on dynamic recrystallized grain size and steady state stress have been investigated in many researches [2,3,8-13]. The aim of this investigation is to examine the nucleation process of DRX as well as the microstructure evolution during progressing of DRX under various deformation conditions for the 316 stainless steel, where the necklace structure reveals.

2. Experimental procedure

The chemical composition of the 316 stainless steel employed in this work is given in Table. 1. This material was supplied with the form of a hot rolled bar with a diameter of 10 mm. Cylindrical samples 5 mm in diameter and 7.5 mm in height were prepared with their axes aligned along the rolling direction. For minimize the coefficient of friction during hot compression testing, glass plates were put into graves (Rastegave) as lubricant.

One-hit hot compression tests were carried out on a dilatometer machine (BAHR Thermoanalyses GmbH) equipped with induction furnace and a vacuum chamber. The samples totally were deformed after preheated at 1150 °C for 15 min in a vacuum chamber. After annealing the grain size was obtained 46 μm by linear intercept method. Then they were cooled to test temperature. Tests were performed at the temperature range of 950-1100 °C with strain rates of 0.01-1s^{-1} to the true strain of 1. Samples were cut along compression direction and were polished electrochemically in a 65% nitric acid solution. In order to minimize the effect of friction on the stress-strain curves the method of Ebrahimi and Najafizadeh were used and it was simplified as described below [14]:

$$\sigma = \frac{P_{ave}}{8b\frac{R}{H}(\alpha - \beta)} \quad (1)$$

Where:

$$\alpha = \left(\frac{1}{12} + \left(\frac{H}{R}\right)^2 \times \frac{1}{b^2}\right)^{3/2}$$

$$\beta = \left(\frac{H}{R}\right)^3 \times \frac{1}{b^3} - \frac{m}{24\sqrt{3}} \times \frac{e^{-b/2}}{\left(e^{-b/2} - 1\right)}$$

σ = true flow stress of material, Pave = external pressure applied to cylinder in compression, b = the barrel parameter, m = constant friction factor, R and

H represents respectively, the values of radius and height of samples during the test,

$$b = 4 \times \Delta R / R \times H / \Delta H$$

$$R' = \frac{R_T + R_m}{2}$$

$$T = \sqrt{\left(3 \times \left(\frac{H_0}{H}\right) \times R^2{}_0 - 2R^2{}_m\right)},$$

$$m = \frac{\frac{R}{H} \cdot b}{\frac{4}{\sqrt{3}} - \frac{2b}{3\sqrt{3}}}$$

Where:

R': average radius of cylinder after deformation, R_T= top radius of deformed sample, R_m=radius at middle height H = height of cylinder after deformation, H_0=initial height of cylinder, R_0= initial Radius of cylinder, ΔH= final height change, ΔR= radius change.

3. Results and Discussion

3.1. Identification of critical strains

The typical stress- strain curves of single-hit compression tests are presented in Figure 2 for 316 stainless steel. One of the aims of this study is to identify the critical strain for the initiation of DRX (ε_c), peak strain (ε_p), inflection strain (ε_i) and the strain corresponding to the onset of steady-state flow (ε_s). The critical point for the initiation of DRX was determined using the method of Najafizadeh and Jonas [13]. In their approach, the initiation of DRX is associated with a point of inflection in the strain hardening rate (θ) vs. flow stress (σ) plot. According to this method, the strain hardening rate was plotted against flow stress, and the third-order equation that best fit the experimental θ-σ data from yield to the peak stress was found for each set of the deformation conditions.

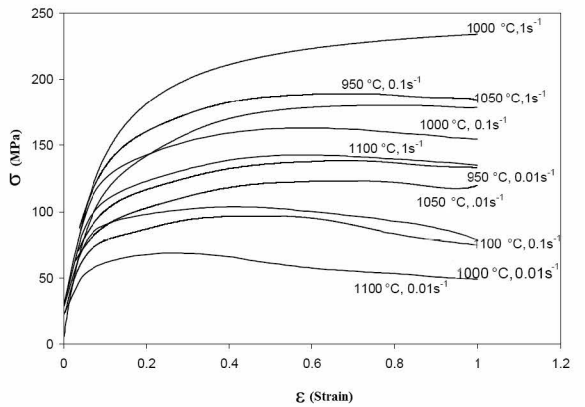

Fig. 2. Stress- strain curves obtained from one-hit compression tests.

The value of ε_c was obtained numerically from the coefficients of the third-order equation. The values of ε_i were identified from the inflection points on the σ-ε curves located between the peak and steady-state stresses. For this purpose, the stress-strain curves were once again fitted using a third-order equation and ε_i was calculated by setting the second derivative of this equation to zero.

3.2. Calculation of the activation energy

The activation energy for deformation was derived with the aid of the following relation between the Zener-Hollomon parameter (Z) and the peak stress (σ_p).

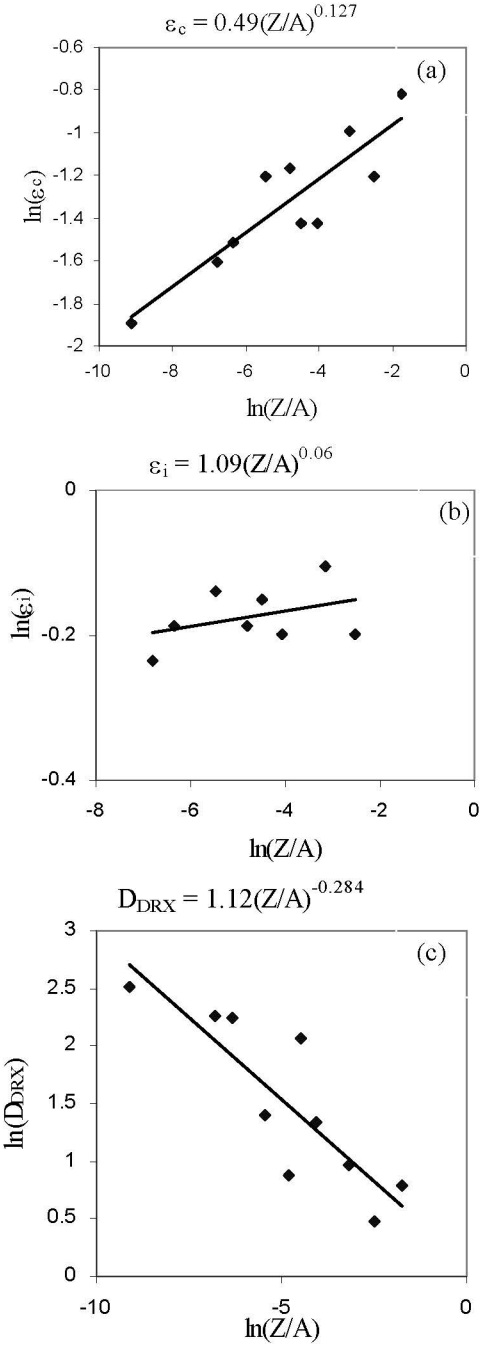

Fig. 3. Relationships between the dimensionless parameter, Z/A and (a) ε_c, (b) ε_i and (c) D_{DRX}.

$$Z = \dot{\varepsilon} \exp\left(\frac{Q_{DRX}}{RT}\right) = A\left[\sinh\left(\alpha\sigma_p\right)\right]^n \quad (2)$$

Therefore,

$$Q_{DRX} = Rn\left(\frac{\partial \ln \sinh\left(\alpha\sigma_p\right)}{\partial\left(\frac{1}{T}\right)}\right)_{\dot{\varepsilon}} \quad (3)$$

Where:

A, α and n = empirical constants, $\dot{\varepsilon}$ is the true strain rate, T = the absolute temperature, Q_{DRX} = the apparent activation energy for deformation, and R = the gas constant. The application of two above equation to the present data resulted in a mean value of Q_{DRX} = 398 (kJ / mol) for the peak stress and A = 1.24×10^{17}. They were obtained by regression analysis.

The dependence of ε_c, ε_i and dynamic recrystallization grain size (D_{DRX}) on the temperature and strain rate in this study can be expressed through power-law relation with dimensionless parameter, Z/A by the following equations.

$$\varepsilon_c = 0.49\left(\frac{Z}{A}\right)^{0.127} \quad (4)$$

$$\varepsilon_i = 0.88\left(\frac{Z}{A}\right)^{0.0108} \quad (5)$$

$$D_{DRX} = 1.12\left(\frac{Z}{A}\right)^{-0.284} \quad (6)$$

The critical strain, ε_c, and the strain at the maximum softening rate, ε_i could be considered with a function of dimensionless parameter, Z/A (Figure 3).

3.3. Necklace mechanism in dynamic recrystallization

As can be seen in Figure 4, dynamic recrystallization developed consecutively by necklace formation at the temperature of 1000 °C and with the strain rate of 0.1 s^{-1}. Figure 4 (a) shows typical annealed twins and bulging which occurred at some parent grain boundaries which presented the beginning of DRX. Figure 4 (b) illustrated the occurrence of a first necklace formation around some grains. Figures 4 (c) and (d) show the expansion of DRX into the grains interior by formation of subsequent layers of necklaces above the steady state strain; however DRX has not yet fully developed into the grain cores.

If DRX proceed into the grains, recrystallization can easily developed over the whole structure by the strain induced boundary migration (SIBM) [2], such condition can be seen in the Figures 5 and 6 in which the microstructure becomes entirely recrystallized. The SIBM is resulted from decreasing the rate of nucleation of DRX grains on pre-existing grain boundaries that maybe due to the large serration. Dynamic recrystallization kinetic can be expressed by Luton and Sellars equation [15-17]:

$$X = 1 - \exp\left(-c\left(\frac{\varepsilon - \varepsilon_C}{\dot{\varepsilon}}\right)^n\right) \quad (7)$$

Where:

n and c can be determined by plotting $LOG(-Ln(1-X))$ vs. $LOG((\varepsilon - \varepsilon_C)/\dot{\varepsilon})$, as shown in Figure 7. The variation of the Avrami exponent (n) can also be associated with the transition from cyclic to single peak of DRX. A high Avrami exponent (~2) is an indication of nucleation on grain edges and twin boundaries, while a low coefficient (~1) indicates that nucleation takes place in the interfacial surface of grains and twin boundaries. In the former case, DRX is controlled by nucleation due to the relatively small number of sites, whereas, at low Avrami exponents, DRX is growth controlled [11,15]. In the present study the Avrami exponent was obtained 1.7 to 2 which indicates to predominant nucleation on grain edges and twin boundaries in all experimental condition that used in this study. The value of the Avrami exponent (n) has the strong effect on the boundary migration mechanism that takes place during DRX.

Not withstanding the fact that the hardness decreases with progress of DRX in common condition, as Figure 8 shows, when the necklace mechanism is predominant in DRX, hardness increases continuously up to the steady state stress. Ponge [4] has been reported this behavior in Ni_3Al due to necklace formation. Such behavior explained by McQueen [1].

According to McQueen [1] the nucleation and growth of new grains are attained by the migration of high angle grain boundary that absorbs existing dislocations leaving behind a region with low dislocation density suitable for source operation. As a new grain grows, multiple sources in the initially formed part can send dislocations into the region behind the advancing grain boundary creating a gradient. This gradient sharpens quite rapidly so that the increased strain energy behind the advancing grain boundary stops the growth, thus determining the grain size. Now due to maintaining an approximately balance between dislocation density in dynamic recrystallized grains and matrix, the growth of advancing grain boundary will be stopped, also dislocation density due to work hardening will be increase. So in necklace structures, hardness will be increased with progression of dynamic recrystallization.

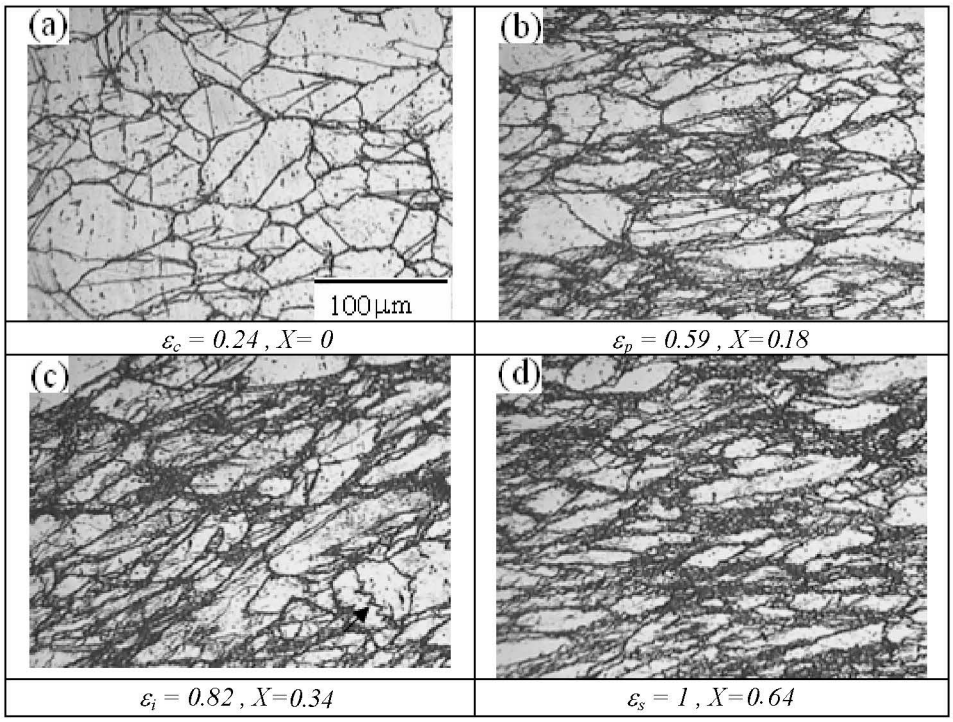

Fig. 4. Microstructural changing at 1000 ℃ with strain rate of 0.1 s^{-1} and at strains of ε_c to ε_s (a)-(d); X denotes dynamic recrystallization fraction in each micrograph.

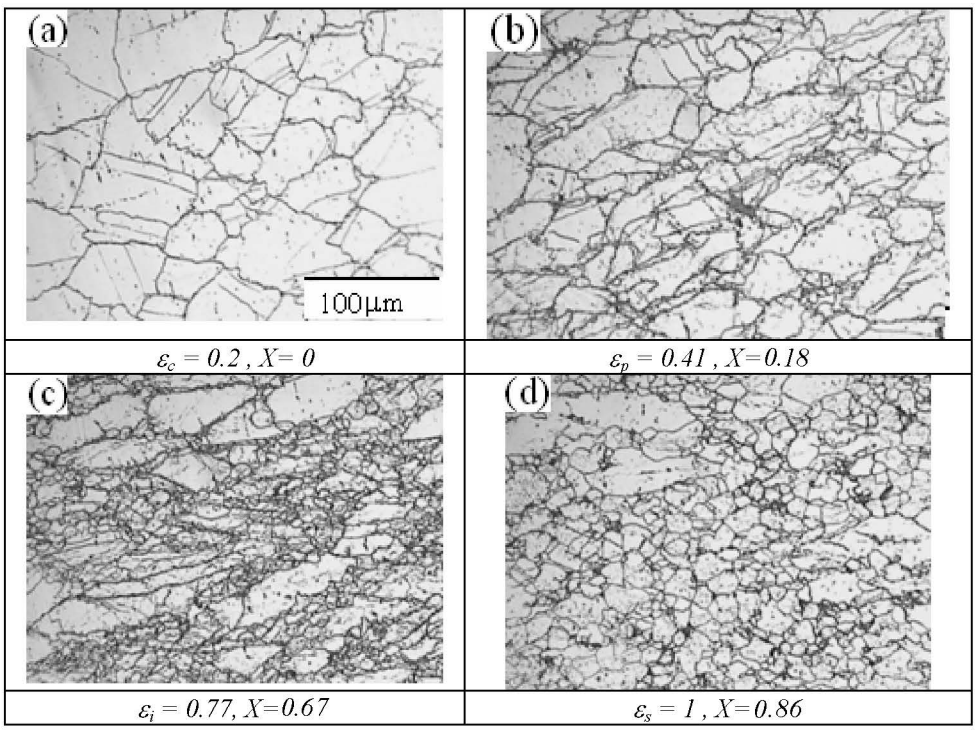

Fig. 5. Microstructural changing at 1100 ℃ with strain rate of 0.1 s^{-1}; Annealed twins can be seen up to the ε_p

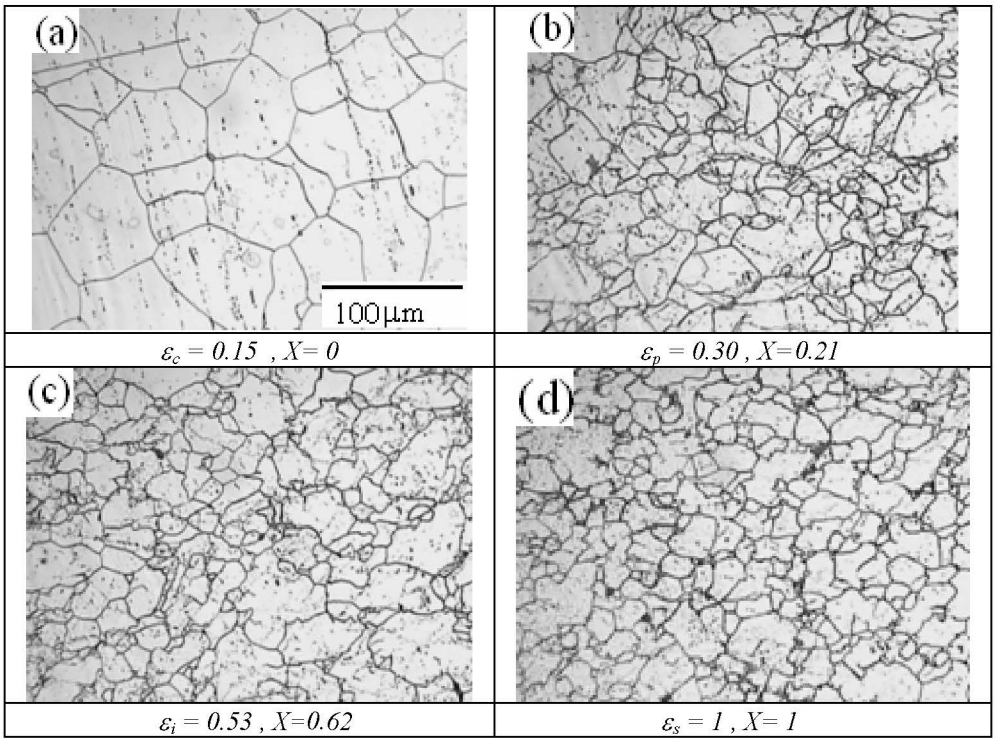

Fig. 6. Microstructural changing at 1100 ℃ with strain rate of 0.01 s^{-1}; dynamic recrystallization is complete by strain up to ε_S.

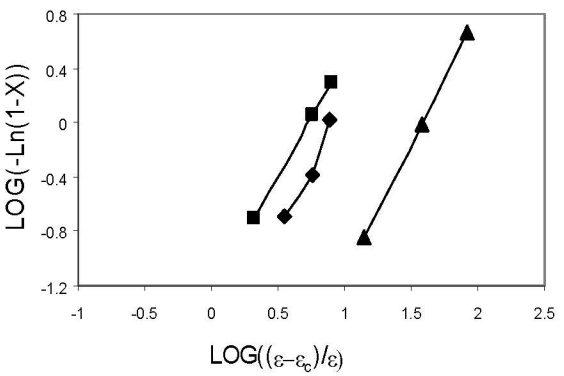

Fig. 7. Dynamic recrystallization kinetic at various conditions.

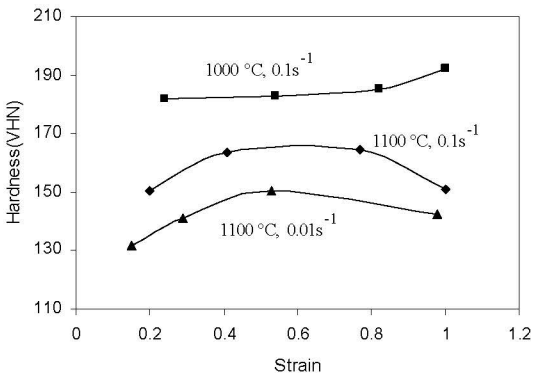

Fig. 8. Variation of hardness versus strain.

Fig. 9 shows microstructures obtained from quenching samples at ε_s in different conditions of deformation. According to these microstructures there were found a good correlation between occurrences of necklacing and Zener-Hollomon parameter that presented in the Table. 2. As can be seen in Figure 9 , necklace structure developed with increasing strain rate at each constant temperature.

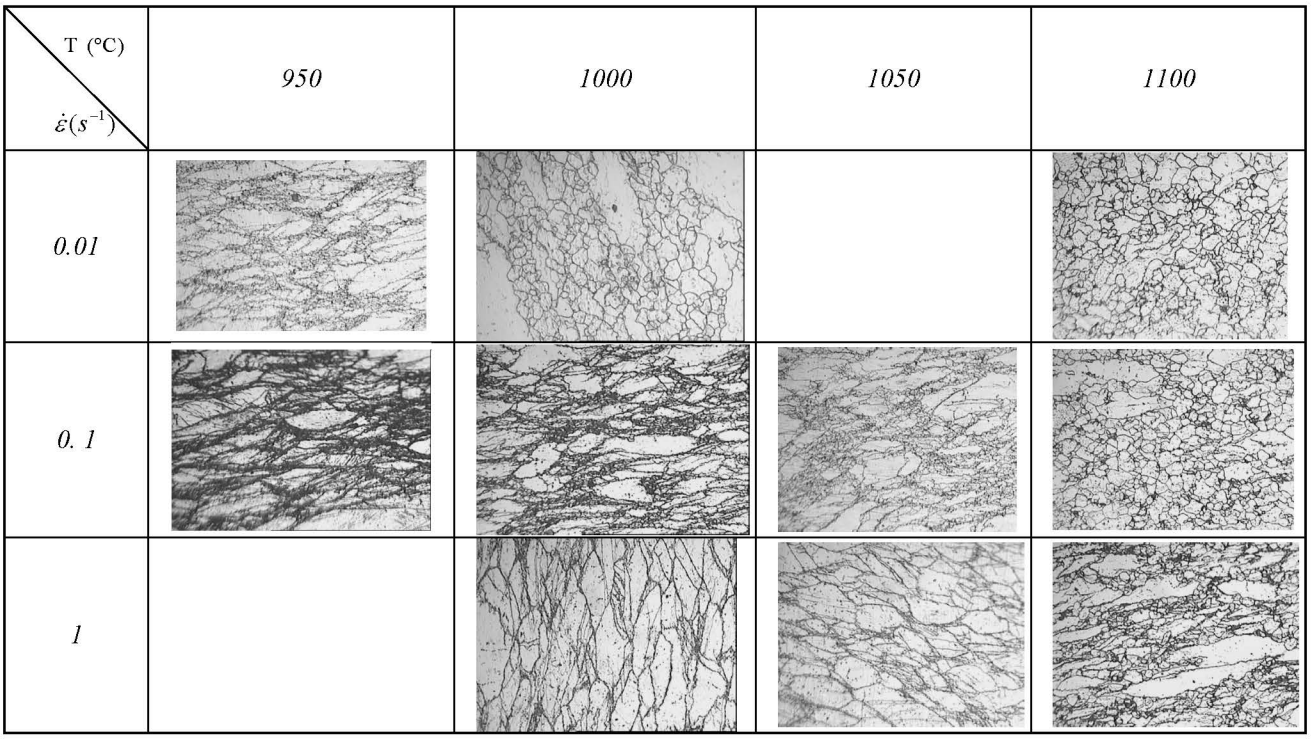

Fig. 9. Microstructural changing obtained from quenching samples at ε_s with different condition of deformation.

Table. 2. Different deformation conditions in which necklace formation can be observed in 316 stainless steel

T (°C)	Strain rate (S^{-1})	Z	Necklace Structure formation
950	0.01	9.98378×10^{14}	Yes
	0.1	9.98378×10^{15}	Yes
	1	9.98378×10^{16}	Yes
1000	0.01	2.14589×10^{14}	No
	0.1	2.14589×10^{15}	Yes
	1	2.14589×10^{16}	Yes
1050	0.01	5.18071×10^{13}	No
	0.1	5.18071×10^{14}	No
	1	5.18071×10^{15}	Yes
1100	0.01	1.38715×10^{13}	No
	0.1	1.38715×10^{14}	No
	1	1.38715×10^{15}	No

Conclusion

The Principal conclusions that can be drawn from the present work are the following:

1- When the necklace mechanism is predominant in DRX, hardness increases continuously up to the steady state.

2- In all experimental condition that used in this study the Avrami exponent was obtained 1.7 to 2 which indicates the predominant nucleation on grain boundaries and twin boundaries.

3- Necklace structure developed with increasing strain rate at each temperature.
4- Very heterogeneous structure comprises of very fine DRX grains and coarse unrecrystallized ones obtained by necklace mechanism.

Acknowledgments

The author expresses theirs thanks to the Center of Excellence for Steel for supporting of this work

References

[1] H. J. McQueen and C.A. Imbert, J. Alloy Compd. 378(2004), 35.
[2] A. Belyakov, Mater. Sci. Eng. A, 255(1998), 139.
[3] D. J. Towel, Metal Sci. (1979), 246.
[4] D. Ponge and G. Gottestein, Acta Mater., 46(1998), 69
[5] W. Roberts, H. Boden and B. Ahblo, Metal Sci. (1979), 195.
[6] Sumantra Mandal, P. V. Sivaprafab, R. K. Dube, International Symposium of Research Students on Material Science and Engineering, (2004), 20-22, Chennai, India.
[7] J. J. Jonas, E. I. Poliak and A. Najafizadeh, Thermec 2006 Vancouver, Canada, Materials Science Forum, (2006), 100.
[8] H. J. McQueen, Mater. Sci. Eng. A, 387–389 (2004), 203.
[9] M. C. Mataya, " Metal. Trans A, 21(1990), 1969.
[10] A. Belyakov, Mater. Sci. Eng. A, 319–321 (2001), 867.
[11] W. Roberts, Metal Sci., (1979), 195.
[12] G. R. Stewart, J. J. Jonas, ISIJ Int., 44(2004), 1581.
[13] A. Najafizadeh and J. J. Jonas, ISIJ Int., 46(2006), 1679.
[14] R. Ebrahimi and A. Najafizadeh, J. Mater. Process. Technol. 152(2004), 136.
[15] Sung-Il Kim, Mater. Sci. Eng. A, 311(2001), 108.
[16] M. El Wahabi, Mater. Sci. Eng. A, 343(2003), 116.
[17] Sung-Il Kim, Mater. Sci. Eng. A, 357(2003), 235.